American Journal of Pathology, Vol. 168, No. 2, February 2006

DOI: 10.2353/ajpath.2006.050372

Vascular Biology, Atherosclerosis and Endothelium Biology

Plasmin Modulates Vascular Endothelial Growth Factor-A-Mediated Angiogenesis during Wound Repair

Detlev Roth,* Michael Piekarek,* Mats Paulsson,†‡ Hildegard Christ,§ Wilhelm Bloch,¶ Thomas Krieg,*‡ Jeffrey M. Davidson,‖** and Sabine A. Eming*

From the Department of Dermatology, the Center for Biochemistry,† Medical Faculty, the Center for Molecular Medicine,‡ the Institute of Medical Statistics, Informatics, and Epidemiology,§ and the Institute for Molecular and Cellular Sport Medicine,¶ University of Cologne, Cologne, Germany; the Department of Pathology,‖ Vanderbilt University School of Medicine, Nashville, Tennessee; and the Veterans Administration Medical Center,** Nashville, Tennessee*

Plasmin-catalyzed cleavage of the vascular endothelial growth factor (VEGF)-A isoform VEGF165 results in loss of its carboxyl-terminal heparin-binding domain and significant loss in its bioactivity. Little is known about the *in vivo* significance of this process. To investigate the biological relevance of the protease sensitivity of VEGF165 in wound healing we assessed the activity of a VEGF165 mutant resistant to plasmin proteolysis (VEGF165^{A111P}) in a genetic mouse model of impaired wound healing (db/db mouse). In the present study we demonstrate that in this mouse model plasmin activity is increased at the wound site. The stability of the mutant VEGF165 was substantially increased in wound tissue lysates in comparison to wild-type VEGF165, thus indicating a prolonged activity of the plasmin-resistant VEGF165 mutant. The db/db delayed healing phenotype could be reversed by topical application of wild-type VEGF165 or VEGF165^{A111P}. However, resistance of VEGF165 to plasmin cleavage resulted in the increased stability of vascular structures during the late phase of healing due to increased recruitment of perivascular cells and delayed and reduced endothelial cell apoptosis. Our data provide the first indication that plasmin-catalyzed cleavage regulates VEGF165-mediated angiogenesis *in vivo*. Inactivation of the plasmin cleavage site Arg110/Ala111 may preserve the biological function of VEGF165 in therapeutic angiogenesis under conditions in which proteases are highly active, such as wound repair and inflammation. ***(Am J Pathol 2006, 168:670–684; DOI: 10.2353/ajpath.2006.050372)***

Vascular endothelial growth factor-A (VEGF-A) is the most potent and specific vascular growth factor and a key regulator in physiological and pathological processes of angiogenic remodeling.[1] VEGF-A levels are regulated through transcriptional control and mRNA stability. Moreover, using differential mRNA splicing, the single human VEGF-A gene can give rise to at least eight isoforms (VEGF121, 145, 148, 162, 165, 183, 189, and 206) whose relative levels vary among different tissues.[1,2] The most abundant isoform found in human tissue is VEGF165. All isoforms contain the binding site for VEGF tyrosine kinase receptors VEGF receptors 1 (VEGFR-1/Flt-1) and 2 (VEGFR-2/KDR/Flk-1), which is encoded by exons 1 to 5.[3] The isoforms are distinguished by the presence or absence of peptides encoded by exons 6 and 7 of the VEGF-A gene encoding two independent heparin-binding domains. Substantial evidence indicates that differences in the expression of the heparin-binding domains are crucially involved in the diverse biochemical and functional properties of the VEGF-A splice forms such as binding to cell surfaces and extracellular matrix,[4–7] receptor binding characteristics,[8] endothelial cell adhesion and survival,[7,9] and vascular branch formation.[10]

In addition to mRNA-splicing, proteolytic mechanisms also generate VEGF-A variants lacking peptides encoded by exon 6 and/or 7, thereby generating

Supported by the Deutsche Forschungsgemeinschaft (grants FOR 265 to S.A.E. and SFB 589 to M.P. and T.K.); the National Institutes of Health (grant AG06528 to J.M.D.); the United States Department of Veterans Affairs (to J.M.D.); and the European Community (LSHB-CT-2005-512102 to S.A.E.).

Accepted for publication October 11, 2005.

Address reprint requests to Priv.-Doz. Dr. med. Sabine A. Eming, Department of Dermatology, University of Cologne, Joseph-Stelzmann Str. 9, 50931 Köln, Germany. E-mail: sabine.eming@uni-koeln.de.

VEGF-A cleavage products with different biological activities.[11–13] This suggests that the proteolytic microenvironment could function as a critical determinant controlling VEGF-A-mediated activities. We and other investigators have demonstrated the sensitivity of VEGF165 to serine proteases, in particular plasmin.[11,12,14,15] Plasmin digestion of VEGF165 yields two fragments: an amino-terminal homodimer (VEGF1-110) containing the VEGF receptor binding site and a carboxyl-terminal polypeptide comprising the heparin-binding domains (VEGF111-165).[12,14,15] Loss of the carboxyl-terminal heparin binding domain through plasmin digestion significantly reduces VEGF165 mitogenic activity on human umbilical vein endothelial cells, supporting the crucial significance of the heparin-binding domains for VEGF-A function.[12,15] So far, little is known about the prevalence and biological significance of proteolytic digestion of VEGF-A *in vivo*.

VEGF-A plays a pivotal role during the angiogenic response in tissue repair, by regulating vascular permeability, the influx of inflammatory cells into the site of injury, migration and proliferation of pre-existing endothelial cells and, as suggested recently, the recruitment of marrow-derived endothelial progenitor cells to the local wound site where they are able to accelerate repair.[16–20] We recently provided evidence that in the highly proteolytic environment of human nonhealing skin ulcers VEGF165 protein degradation is increased as compared to normal-healing wounds.[14] Protease inhibitor studies and increased stability of a plasmin-resistant VEGF165 mutant after exposure to wound fluid of nonhealing human chronic wounds indicated that plasmin is one of the serine proteases critically involved in this process.[15] Hence, plasmin-catalyzed VEGF165 proteolysis and inactivation may lead to reduced VEGF165 availability at the wound site and contribute to an impaired healing response. To further characterize the biological relevance of the protease sensitivity of VEGF165 during cutaneous repair, in the present study we tested the stability and activity of a locally applied VEGF165 mutant resistant to plasmin proteolysis ($VEGF165^{A111P}$) in a genetic mouse model of impaired healing (db/db mouse). Our experiments provide the first *in vivo* data indicating that plasmin-catalyzed cleavage is critical to regulate VEGF165-mediated angiogenesis. Our data indicate that inactivation of the plasmin cleavage site Arg110/Ala111 increases the overall integrity of the VEGF165 molecule with significant consequences to blood vessel persistence.

Materials and Methods

Plasmids

Plasmid DNA encoding human wild-type VEGF165 (CMV-VEGF165-Wt) or a plasmin-resistant VEGF165 mutant $VEGF165^{A111P}$ (CMV-$VEGF165^{A111P}$) was generated as previously described.[15] Briefly, mutagenesis was performed using a base mismatched oligonucleotide as indicated: 5′-GACCAAAGAAAGATAGACCAAGACAAG-3′ (nucleotide difference between wild-type VEGF165 and mutant is underlined) (MWG-Biotech, Ebersberg, Germany). This mutation results in the substitution of alanine at position 111 by proline and yields a plasmin-resistant and biologically active VEGF165 molecule as demonstrated recently.[15] $VEGF165^{A111P}$ was generated using the Gene-Editor *in vitro* site-directed mutagenesis system (Promega, Mannheim, Germany). A cDNA encoding human VEGF165-Wt or $VEGF165^{A111P}$ was ligated into the *Bam*H1 and *Eco*R1 sites of the expression plasmid pcDNA 3.1 (Invitrogen, De Schelp, The Netherlands) containing a cytomegalovirus (CMV) promoter. To follow VEGF165 transgene expression *in vivo* a VEGF165-Wt-myc-his fusion protein was generated. A cDNA coding for VEGF165-Wt was inserted into a pcDNA 3.1 myc-his expression plasmid containing a CMV promoter (Invitrogen); the myc-tag was added to the carboxyl-terminus of the VEGF165 molecule. The β-galactosidase expression plasmid containing a cytomegalovirus promoter (CMV-LacZ) was a gift from Dr. M. Hafner (National Research Center for Biotechnology, Braunschweig, Germany). The sequences of expression constructs were verified by DNA sequencing. Plasmids were propagated in *Escherichia coli* DH1α, and plasmid DNA was prepared on Qiagen chromatographic columns as recommended by the manufacturer (Qiagen Plasmid midi kit; Qiagen, Hilden, Germany).

Isolation of VEGF165 Proteins

VEGF165-proteins were generated and fractionated as recently described.[15] Briefly, COS-1 cells were transfected using the Superfect transfection reagent (Qiagen) following the manufacturer's instructions. Conditioned medium was incubated with heparin-Sepharose (Amersham Bioscience, Braunschweig, Germany) and was packed in a column. Elution of bound proteins was performed by 10 mmol/L Tris-HCl, pH 7.2, 0.9 mol/L NaCl. Fractions were pooled, desalted (D-Salt Excellulose plastic desalting columns; Pierce, St. Augustin, Germany), lyophilized, and the concentration of VEGF165 was determined using a commercially available hVEGF165-specific enzyme-linked immunosorbent assay (R&D Systems, Minneapolis, MN). The assay was performed following the manufacturer's instructions. The mitogenic activity of both VEGF165 variants was similar when tested on human umbilical vein endothelial cells.[15] Because VEGF165 proteins were purified by heparin-Sepharose they are termed partially purified VEGF.

Gene Transfer

Cutaneous transfections were performed as described previously using the Bio-Rad Helios delivery device (Bio-Rad, München, Germany).[21–23] Briefly, supercoiled plasmid DNA was precipitated onto gold particles (0.95 mm in diameter) in the presence of 50 mmol/L spermidine and 0.5 mol/L $CaCl_2$ at a concentration of 5 μg of DNA per mg of gold. The DNA/gold complexes were washed with absolute ethanol and resuspended in absolute ethanol. The suspension was used to coat the interior of

1/8-inch Tefzel tubing (Bio-Rad) in a specially designed apparatus (Bio-Rad). After the particles adhered to the tubing, it was cut into 1/2-inch lengths such that 0.25 mg of DNA/gold complexes would be delivered with each shot. DNA/gold particles were accelerated into the tissue surface by the rapid release of a pulse of helium at 300 psi.

RNA Isolation and Reverse Transcriptase-Polymerase Chain Reaction (RT-PCR)

Total RNA was isolated from transfected skin by the guanidine isothiocyanate-acid phenol method. Residual plasmid DNA was destroyed by digestion of the RNA preparation with 1 U per RNase-free deoxyribonuclease (30 minutes, 37°C). To generate cDNA, RNA was reverse-transcribed using Superscript reverse transcriptase and oligo $(dT)_{12\text{-}18}$ primers (Life Technologies, Gibco BRL, Eggenstein, Germany). The reaction mixture was incubated for 1 hour at 42°C and chilled on ice. The RNA template was hydrolyzed by digesting the reaction product with RNaseH before amplification. Portions of 1/10 vol of the first-strand synthesis reaction were then amplified by 30 cycles of PCR for VEGF164/165 or GAPDH adding primers specific for either VEGF164/165 (EMBL, accession no. M32977) (5′-GAGTCCAACATCACCATGCAG-3′, 5′-TCACCGCCTTGGCTTCTCACA-3′), or GAPDH (EMBL, accession no. M33197) (5′-TCATGACCACAGTCCATGCCATCA-3′, 5′-GCCAAATTCGTTGTCATACCAGGAAATGA-3′) (MWG Biotech) using a Thermocycler (Trio-Thermocycler; Biometra, Göttingen, Germany). The primers were chosen such that only the resulting amplification product of the transfected human VEGF165 would contain the *Dde*I endonuclease site. The amplified products were digested with *Dde*I, size fractionated by electrophoresis in a 2% TBE-agarose gel, transferred to a nitrocellulose membrane (Hybond-N, Amersham), and subjected to Southern blot hybridization with a random-primed ^{32}P-dCTP-labeled VEGF probe (Ladderman labeling kit; Takara Bio Inc., Shiga, Japan).

Animals

C57BLKS/J-m+/+Lepr^{db} (db/db) and C57BL/6 mice were maintained and bred in the animal care facility of the Center for Molecular Medicine, University of Cologne, (Cologne, Germany). Genotyping of db/db mice was achieved by PCR analysis; primers were chosen so that the PCR product contains the db/db mutation that leads to loss of the *Rsa*I restriction site in exon 12 (EMBL, accession no. MMU58861) (5′-AGAACGGACACTCTTTGAAGTCTC-3′, 5′-CATTCAAACCATAGTTTAGGTTTGTGT-3′). Male mice were 10 to 12 weeks of age at the start of the experiments.

Wounding

Four independent wound-healing experiments were performed; mice were anesthetized under Ketanest/Rompun (Ketanest S from Park Davies GmbH, Karlsruhe, Germany, and Rompun 2% from Bayer, Leverkusen, Germany). The animals' backs were shaved and four full-thickness punch-biopsy wounds (6 mm in diameter and 5 mm apart) were created. Wounds were either created immediately after transfection within the transfected target side or created in nontransfected skin and treated daily from day 1 through day 7 after injury with recombinant human VEGF165 protein (rhVEGF165) (1 μg in 100 μg of methylcellulose) or methylcellulose (control) (Intra-Site Gel; Smith and Nephew, Lohfelden, Germany) and covered with a semiocclusive dressing. Treatment of wounds was rotated among sites to avoid site-specific bias. Analysis of wound closure was achieved through digital processing of photographs taken daily during the time of healing using the Imaging Software Lucia G 4.80 (Dental Eye, Olympus, Japan and Imaging Software Lucia G 4.80 from Laboratory Imaging Ltd., Prague, Czech-choslovakia); wound closure was calculated as the percentage of the wound area at day 1 after wounding. For histological analysis animals were sacrificed and wounds were harvested at 1, 3, 5, 8, 11, 12, 15, and 18 days after wounding. An area of 8 μm in diameter, which includes the complete epithelial margins, was excised at each time point; wounds were cut exactly in half and embedded in OCT compound (Tissue Tek; Miles, Elkhart, IN), immediately frozen in liquid nitrogen, and stored at −80°C. Complete histological analysis was performed on serial sections (5-μm cryosections) from the central portion of the wound.

Analysis of Wound Re-Epithelialization and Granulation Tissue Formation

The extent of re-epithelialization and granulation tissue formation was measured by histomorphometric analysis of tissue sections (hematoxylin and eosin stain) using the Imaging Software Lucia G 4.80. For analysis of re-epithelialization, the distance that the epithelium had traveled across the wound was measured; the muscle edges of the panniculus carnosus were used as indicator for the wound edges; re-epithelialization was calculated as the percentage of the distance of muscle edges of the panniculus carnosus. For the quantification of granulation tissue, the wound site was identified, outlined, and the area covered by a highly cellular and vascularized tissue was determined. All histomorphometric analyses were performed blinded by two independent investigators.

Immunohistochemistry and Morphometric Quantification

To process tissue sections for the immunodetection of CD31 (PECAM-1) (eight wounds per time point), VEGFR-2 (eight wounds per time point), F4/80 (five wounds per time point), or the fusion protein VEGF165-Wt-myc (three wounds per time point), 5-μm cryosections were fixed in acetone, endogenous peroxidase was blocked (0.03% H_2O_2, 0.15 mol/L NaN3), and samples

were then blocked with 3% bovine serum albumin in phosphate-buffered saline (PBS). Sections were incubated with polyclonal rat antisera against murine CD31 (1 hour at room temperature, 1:500) (Pharmingen, Heidelberg, Germany), murine VEGFR-2 (1 hour at room temperature, 1:200) (Pharmingen), murine F4/80 (24 hours at 4°C, 1:10) (Serotec, Eching, Germany), or myc (1 hour at room temperature, 1:500) (Invitrogen). Bound primary antibodies were detected using a peroxidase-conjugated goat anti-rat antibody (Southern Biotechnology, Birmingham, AL). 3-Amino-9-ethyl-carbazol was used as a substrate, and sections were counterstained with hemalaun. As a control for specificity, primary antibodies were omitted and replaced by an irrelevant isotype-matched rat antibody. For semiquantitative analysis of immunohistochemical staining, video images of at least three serial wound sections per wound were captured and analyzed using the Imaging Software Lucia G 4.8; data are expressed as percentage of granulation tissue area. To determine average vessel size in CD31-stained sections, the capillary lumen was examined in three different fields on each wound section at a 400-fold magnification. All histomorphometric analysis was performed blinded by two independent investigators. To detect LacZ gene expression, cryosections were processed as described recently.[24]

Detection of Plasmin Activity

The presence of plasmin activity during wound repair was analyzed in lysates prepared from wound tissue. Wounds were harvested at 1, 3, 5, 8, and 14 days after wounding; an area of 8 mm in diameter, which includes the complete epithelial margins, was excised at each time point. Wound tissue was immediately frozen in liquid nitrogen and stored at −80°C until use. The frozen tissue was powdered and resuspended in 200 μl of buffer (50 mmol/L Tris, pH 7.8). The tissue was disrupted by sonication for 10 seconds at 50 W and the suspension was centrifuged (5 minutes at 15,000 × *g*). Plasmin activity was quantified in the supernatant using a fluorescent assay based on a plasmin-specific substrate; the difference in fluorescence between the substance formed by plasmin cleavage and the original nonfluorescent substrate is determined (H-D-Val-Leu-Lys-AMC) (Bachem, Heidelberg, Germany). Lysates generated from individual wounds were analyzed. To determine substrate-degrading enzymes, α2-antiplasmin (0.7 IU/ml) (Sigma, Deisenhof, Germany) was added. Plasmin activity was normalized to total protein concentration.

Sodium Dodecyl Sulfate-Polyacrylamide Gel Electrophoresis (SDS-PAGE) and Immunoblotting

SDS-PAGE was performed following the protocol of Laemmli. VEGF165 variants (5 ng) expressed in COS-1 cells were incubated at 37°C with wound tissue lysates obtained from db/db mice 3, 5, 8, and 14 days after injury. Reactions were terminated by the addition of Pefabloc (1 mmol/L) and frozen at −20°C. To identify VEGF165-degrading enzymes, α2-antiplasmin (0.7 IU/ml) was added to wound lysates 30 minutes before VEGF165 protein incubation. For Western blotting fragments were resolved on 12% nonreducing SDS-PAGE gels and transferred to nitrocellulose (Hybond C-Super, Amersham Biosciences). VEGF165 amino terminal integrity was determined by detecting immunoreactive products with a polyclonal rabbit antibody that recognizes the amino-terminal VEGF epitopes (raised against a 20-amino acid amino-terminal peptide; Santa Cruz Biotechnology, Santa Cruz, CA). Detection of intact and VEGF165-derived degradation products was accomplished using the LumiLight plus chemiluminescence detection system (Roche Diagnostics, Mannheim, Germany). Densitometric analysis of Western blots was performed using a FluroS-Multiimager and Quantity One analysis software (Bio-Rad).

Immunofluorescent Staining

All immunofluorescent staining was performed on 5 μm cryosections; particular caution was taken to store and treat all tissues and tissue sections equally. Terminal dUTP nick-end labeling (TUNEL) staining was performed with a commercial kit (DeadEnd Fluorometric TUNEL System; Promega, Madison, WI) following the instructions of the manufacturer. After TUNEL staining sections were fixed in paraformaldehyde (1% in PBS) and rinsed, and immunodetection of CD31 was performed as described above. Bound primary antibody was detected using an Alexa Fluor 594-conjugated polyclonal goat anti-rat antibody (1 hour, 1:500) (Molecular Probes, Leiden, The Netherlands). As a control for positive TUNEL staining the TDT enzyme was omitted. Immunofluorescent microscopy was conducted at ×600 magnification (Eclipse 800E; Nikon, Düsseldorf, Germany); images were captured with a digital camera (DXM1200 F; Nikon) and Imaging Software Lucia G4.8. Endothelial cells were identified by red fluorescence, and DNA fragmentation was detected by localized green fluorescence within the nucleus of apoptotic cells. Apoptotic endothelial cells were counted in three individual fields per wound, and serial sections were analyzed (CMV-VEGF165-Wt wounds, $n = 4$; CMV-VEGF165^{A111P} wounds, $n = 4$). To detect the presence of endothelial cells and pericytes, immunodetection of CD31 was performed as described above; detection of α-smooth muscle actin (α-SMA) or desmin for pericytes was performed using an antiserum Cy3-conjugated murine anti-α-SMA (1 hour, 1:200) (Sigma) or a monoclonal IgG1 mouse anti-desmin (24 hours at 4°C, 1:200) (Dako Cytomation GmbH, Hamburg, Germany). Bound primary antibody was detected using an Alexa Fluor 488-conjugated polyclonal goat anti-mouse IgG1 antibody (1 hour, 1:500) (Molecular Probes); double fluorescence was analyzed in a laser-scanning confocal microscope at ×400 magnification (True Confocal Scanner Leica TCS SL; Leica Microsystems Heidelberg GmbH, Heidelberg, Germany). For quantitative analysis of immunohistochemical staining video images

of at least three serial wound sections per wound were captured and the stained area was analyzed using the Imaging Software Lucia G 4.8. All analyses were performed blinded by two independent investigators.

Statistical Analysis

Statistical analyses were performed using the SigmaStat program 12.0.2 (SPSS GmbH, München, Germany). An analysis of variance was applied and followed by *t*-tests for comparisons in pairs. All data are presented as mean ± SD. A *P* value less than 0.05 was considered significant.

Results

In Vivo *Transgene Expression*

To examine the biological effects of transient, local expression of VEGF165-Wt and VEGF165^{A111P} transgene on tissue repair *in vivo*, we used particle-mediated gene delivery to transfect the back skin of mice with CMV-VEGF165-Wt, CMV-VEGF165^{A111P}, or CMV-LacZ expression constructs. Particle bombardment is a physical method for gene delivery, and in earlier studies we and others have demonstrated the efficacy of this technology for cutaneous *in vivo* gene transfer in different animal model systems.[22–24] In murine skin maximal transgene expression was correlated with a driving pressure of 300 psi that caused particles to accumulate just above the dermal-epidermal junction with a minor population of particles seen within the dermis (Figure 1C). To determine transgene expression, total RNA was isolated from transfected tissue sites and subjected to reverse-transcription using VEGF-A-specific oligonucleotide primers, generating a 286-bp PCR product (Figure 1A). In humans, but not in mice, this product contains a unique *Dde*I restriction site. RT-PCR reactions were analyzed by Southern blotting with ^{32}P-labeled human VEGF-A cDNA. Endogenous mouse VEGF-A reaction product was detected at 286 bp, whereas the *Dde*I-cleaved human products migrated at 142 bp and 144 bp (Figure 1B). Human transgene expression was detected up to 7 days after transfection. Thus, tissues transfected by particle bombardment are capable of expressing appropriate mRNA. As indicated by the X-Gal stain, keratinocytes represent the majority of transfected cells (Figure 1C1). To follow the secreted VEGF165 transgene product we generated a VEGF165-Wt-myc fusion protein and transfected skin with the corresponding CMV-VEGF165-Wt-myc expression construct. As demonstrated by immunohistochemical staining for the myc epitope, expression of the VEGF165 fusion protein could be detected in the epidermis and in a small number of positive dermal cells. The positive staining of the fusion protein in the extracellular space beneath the transfected epithelium indicates that the fusion protein was released by transfected cells in the upper dermis (Figure 1, C2 and C3).

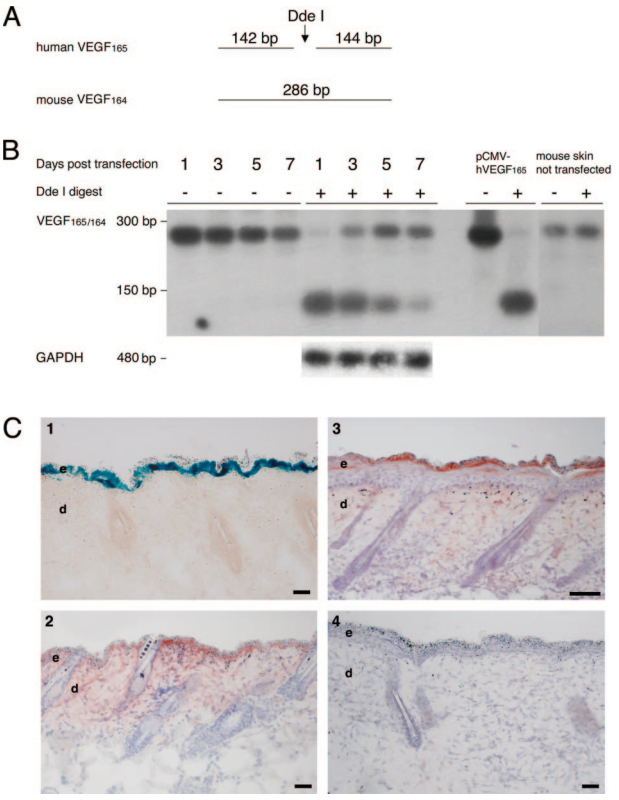

Figure 1. VEGF165 transgene expression *in vivo* after particle bombardment. Back skin of db/db mice was transfected with a CMV-VEGF165-Wt expression construct. To follow transgene expression, total RNA was isolated at indicated time points after transfection and subjected to RT-PCR using VEGF165-specific oligonucleotide primers. **A:** The PCR product of both species is 286 bp; in the human this product is cleaved by *Dde*I into 142-bp and 144-bp products. **B:** The digestion products of the RT-PCR reaction were analyzed by gel electrophoresis and detected by Southern blotting with a ^{32}P-labeled VEGF165 cDNA. The endogenous mouse VEGF164 reaction product is detected at 286 bp, whereas the cleaved human products migrate at 142 bp and 144 bp. RT-PCR of GAPDH and detection of the reaction product by Southern blotting with a ^{32}P-labeled GAPDH cDNA served as a positive control. **C:** Keratinocytes present the majority of transfected cells with a small number of particles present in the epidermis of positive cells noted in the upper dermis; note gold and upper dermis; CMV-LacZ gene expression visualized by X-Gal staining 3 days after transfection (**1**); CMV-VEGF165-Wt-myc gene expression visualized by myc-staining 3 (**2**) and 5 (**3**) days after transfection; the fusion protein (red staining) is expressed in the epidermis and is released in the upper dermis; control for myc-staining (**4**). Scale bars, 100 μm.

Topically Applied rhVEGF165 Protein or Transfection with CMV-VEGF165-Wt Expression Constructs Accelerates Wound Closure

Analysis of the wound closure rate demonstrates that rhVEGF165 protein treatment of wounds in db/db mice significantly accelerated wound closure when compared to control wounds treated with methylcellulose (Figure 2A) ($P < 0.004$). When compared to methylcellulose-treated wounds in C57BL/6 mice, wound closure analysis shows that rhVEGF165 protein treatment of wounds in db/db mice nearly reversed the delayed healing phenotype to normal healing (Figure 2A). To examine the biological effect of transient, local expression of CMV-VEGF165-Wt on tissue repair, we used particle-mediated gene delivery to transfect the skin of

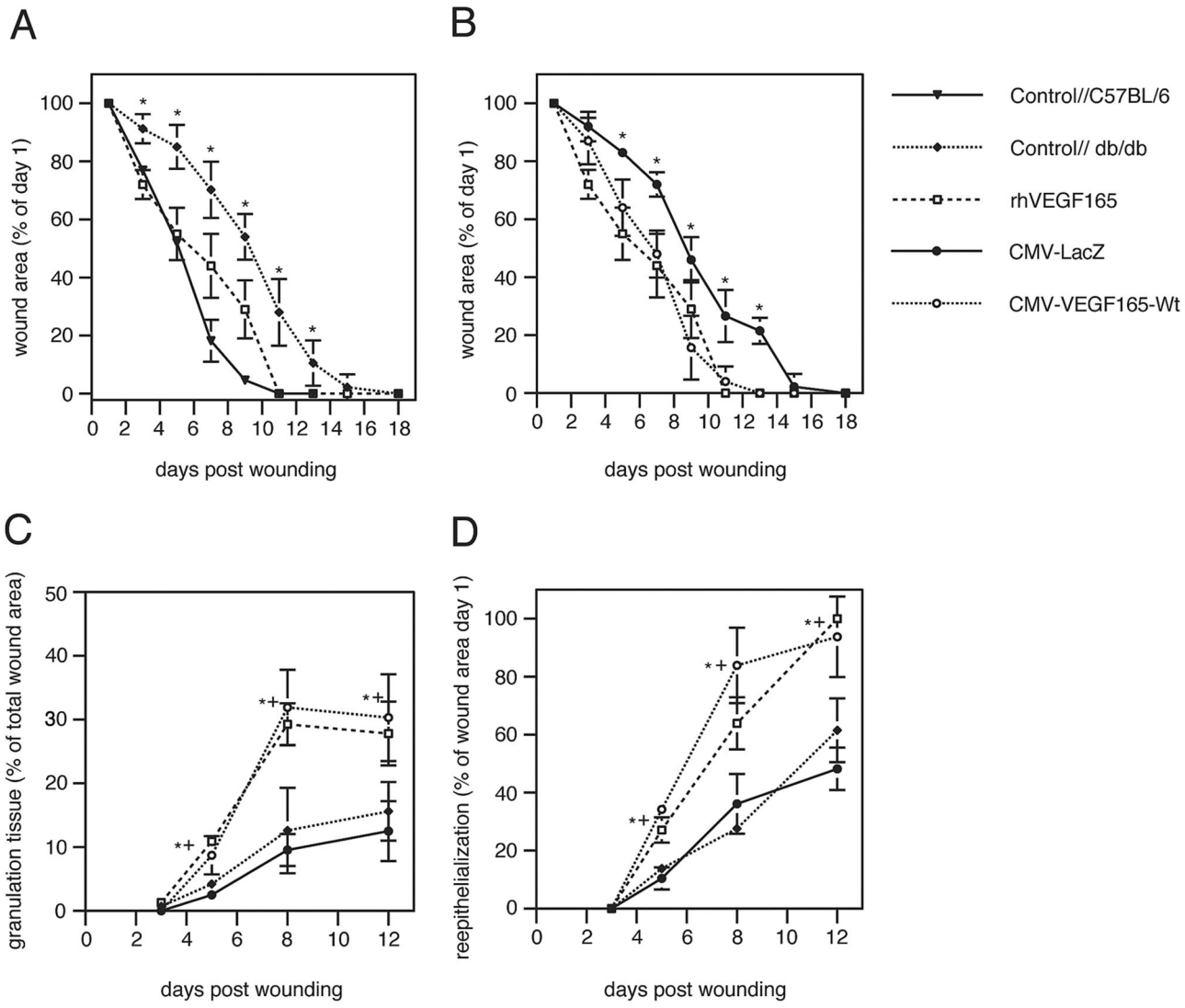

Figure 2. Topically applied rhVEGF165 protein or transfection with CMV-VEGF165-Wt expression constructs accelerates wound closure of full-thickness wounds in db/db mice. **A:** Wounds in db/db mice treated with rhVEGF165 protein or methylcellulose (control//db/db); wounds in C57BL/6 mice were treated with methylcellulose only (control//C57BL/6) (rhVEGF165 versus control//db/db, $^{*}P < 0.004$). **B:** Wounds in db/db mice transfected with CMV-VEGF165-Wt or CMV-LacZ expression constructs (CMV-VEGF165-Wt versus CMV-LacZ, $^{*}P < 0.02$). **C:** Granulation tissue formation in rhVEGF165 protein or methylcellulose-treated (control//db/db) or CMV-LacZ- or CMV-VEGF165-Wt-transfected wounds in db/db mice (rhVEGF165 versus control//db/db, $^{*}P < 0.03$; CMV-VEGF165-Wt versus CMV-LacZ, $^{+}P < 0.03$). **D:** Re-epithelialization in rhVEGF165 protein- or methylcellulose-treated (control//db/db) or CMV-LacZ- or CMV-VEGF165-Wt-transfected wounds in db/db mice (rhVEGF165 versus control//db/db, $^{*}P < 0.01$; CMV-VEGF165-Wt versus CMV-LacZ, $^{+}P < 0.02$). Wounds are $n = 8$/time point for each treatment modality; data are expressed as mean ± SD.

db/db mice with cDNA encoding the corresponding gene. As compared with control wounds transfected with a CMV-LacZ expression construct, VEGF165-Wt transgene significantly enhanced wound closure (Figure 2B) ($P < 0.02$). In nearly all CMV-VEGF165-Wt-transfected wounds wound closure was completed by day 11 after injury, whereas complete wound closure in CMV-LacZ-transfected control wounds was achieved at the earliest by day 15 after injury. Morphometric analysis of granulation tissue indicated that application of either rhVEGF165 protein or CMV-VEGF165-Wt transfection significantly increased the formation of granulation tissue during healing when compared to control wounds treated with methylcellulose or transfected with a CMV-LacZ construct (Figure 2C) (rhVEGF165 versus control//db/db, $P < 0.03$; CMV-VEGF165-Wt versus CMV-LacZ, $P < 0.05$). At high magnification erythrocytes were present in the vessel lumen indicating the functionality and integrity of vascular structures. In addition, increased re-epithelialization also contributed to improved wound closure in VEGF165-treated wounds. Re-epithelialization occurred rapidly in rhVEGF165 protein-treated, or CMV-VEGF165-Wt-transfected wounds, with an average of 50% epithelialization on day 7 after injury (Figure 2D). In contrast, methylcellulose-treated or CMV-LacZ-transfected control wounds showed significantly delayed re-epithelialization, averaging 50% on day 11 after healing (Figure 2D). The accelerated wound-healing response was similar in wounds transfected once with CMV-VEGF165-Wt cDNA, in comparison to wounds treated topically with a daily application of

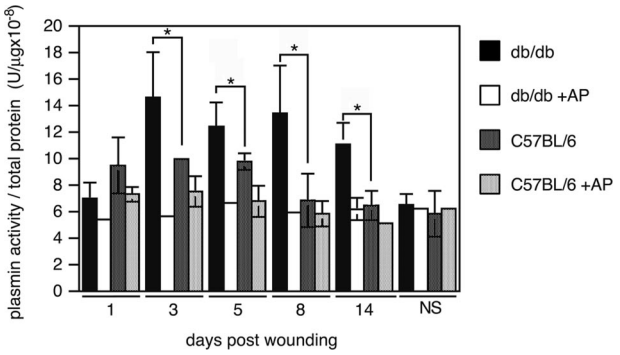

Figure 3. Plasmin activity is increased in db/db wound tissue lysate. Time course of plasmin activity in wound tissue lysates of db/db or C57BL/6 mice with or without α2-antiplasmin. Unwounded skin (NS) served as control. Wounds are $n = 5$/time point; data are expressed as mean ± SD (db/db versus C57BL/6, $^*P < 0.05$).

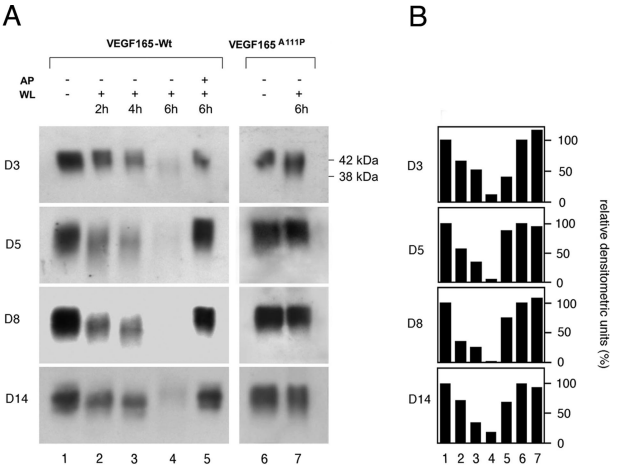

Figure 4. Stability of VEGF165^{A111P} protein is increased in db/db wound tissue lysate. **A:** VEGF165-Wt (**lanes 2** to **5**) or VEGF165^{A111P} (**lanes 6** and **7**) protein was incubated with wound tissue lysates (WL) harvested from db/db mice at indicated time points after wounding (days 3 to 14), for increasing time periods as indicated (2 to 6 hours). α2-Antiplasmin (AP) could partially inhibit VEGF165-Wt degradation (**lane 5**). Degradation of VEGF165 variants was monitored by SDS-PAGE under nonreducing conditions. **B:** Degradation of VEGF165 variants incubated in wound tissue lysates was monitored by analyzing the intensity of the 42-kd signal by scanning densitometry and is presented as a percentage of the signal intensity before incubation into wound tissue lysate (**A**, **lane 1**). Lane numbers in **B** correspond to the lane numbers presented in **A**.

rhVEGF165 protein for 7 days after injury (Figure 2, B–D). These results confirm previous findings demonstrating that particle-mediated cutaneous *in vivo* transfection results in an accelerated healing response comparable with that obtained with the topical application of the corresponding recombinant growth factor.[21–23]

Plasmin Activity Is Increased in the db/db Wound Lysate

To investigate the biological relevance of the plasmin sensitivity of VEGF165 during wound repair we assessed the plasmin activity in wound tissue lysates of db/db and C57BL/6 wild-type mice at different time points during repair. In both mouse strains plasmin activity was upregulated during wound repair as compared to nonwounded skin. Proteolytic activity detected in wound tissue lysates was significantly inhibited by α2-antiplasmin, confirming the specificity of plasmin activity measured (Figure 3). Interestingly, in db/db mice plasmin activity at days 3, 5, 8, and 14 after wounding was significantly increased when compared to the activity in C57BL/6 wild-type mice (Figure 3) ($P < 0.05$).

Stability of VEGF165^{A111P} Protein Is Increased in db/db Wound Lysate

To analyze the proteolytic sensitivity of VEGF165 variants in wound beds, recombinant wild-type and mutant VEGF165 proteins were incubated in lysates prepared from wound tissues of db/db mice at indicated time points after injury. As shown by Western blotting, VEGF165 expressed in COS-1 cells appeared as a band migrating at ~42 kd (Figure 4A). Incubation of VEGF165-Wt protein in tissue lysates up to 4 hours resulted in the disappearance of the 42-kd protein leading to a faint protein smear over 42 and 38 kd (Figure 4A). We recently demonstrated that plasmin digestion of VEGF165-Wt resulted in the degradation of the 42-kd protein into a fragment of 38 kd.[15] Prolonged incubation in wound tissue lysates up to 6 hours led to almost complete loss of VEGF165-Wt fragment detection. α2-Antiplasmin was found to inhibit partially the degradation of VEGF165-Wt in wound tissue lysates, indicating that plasmin contributes to VEGF165-Wt degradation during wound repair in db/db mice. Interestingly, the stability of the plasmin-resistant mutant VEGF165 protein in wound tissue lysate was significantly increased when compared to the wild-type protein. Even after a 6-hour incubation, the 42-kd protein band was easily detectable (Figure 4A). Quantification of the Western blots confirmed that the VEGF165 mutant was indeed more resistant to wound tissue lysate proteolytic activity than the VEGF165-Wt (Figure 4B). This data suggests that the plasmin cleavage site Arg110/Ala111 is rate-limiting for the integrity of the carboxyl-terminal domain comprising the heparin-binding domain and in addition for the overall stability of the VEGF165 molecule during wound repair.

VEGF165^{A111P} Accelerates Wound Closure

To investigate the biological relevance of the protease sensitivity of VEGF165 during wound repair we assessed the wound healing and angiogenic activity of a VEGF165 mutant resistant to plasmin proteolysis in db/db mice. As shown earlier and in the present study, particle-mediated *in vivo* transfection of a CMV-VEGF165-Wt construct resulted in a biological response that was comparable with that obtained with the application of recombinant VEGF165 wild-type protein.[21–23] Thus, we used particle-mediated transfection to overexpress the plasmin-resistant VEGF165 mutant in wounds of db/db mice. Analysis of the wound closure rate revealed that the plasmin-resistant VEGF165 mutant was as effective as the wild-type to accelerate the healing response (Figure 5A)

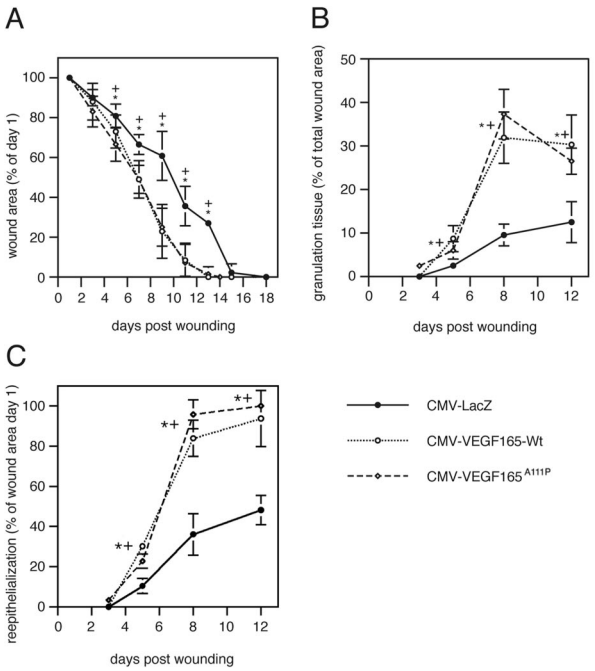

Figure 5. VEGF165^{A111P} accelerates wound closure. **A:** Wounds in db/db mice transfected with CMV-VEGF165-Wt, CMV-VEGF165^{A111P}, or CMV-LacZ expression constructs (CMV-VEGF165-Wt versus CMV-LacZ, $^{*}P < 0.02$; CMV-VEGF165^{A111P} versus CMV-LacZ, $^{+}P < 0.05$). **B:** Granulation tissue formation in CMV-LacZ-, CMV-VEGF165-Wt-, or CMV-VEGF165^{A111P}-transfected wounds in db/db mice (CMV-VEGF165-Wt versus CMV-LacZ, $^{*}P < 0.05$; CMV-VEGF165^{A111P} versus CMV-LacZ, $^{+}P < 0.05$). **C:** Re-epithelialization in CMV-LacZ-, CMV-VEGF165-Wt-, or CMV-VEGF165^{A111P}-transfected wounds in db/db mice (CMV-VEGF165-Wt versus CMV-LacZ, $^{*}P < 0.02$; CMV-VEGF165^{A111P} versus CMV-LacZ, $^{+}P < 0.05$). Wounds are $n = 8$/time point for each treatment modality; data are expressed as mean ± SD.

(CMV-VEGF165-Wt versus CMV-LacZ, $P < 0.02$; CMV-VEGF165^{A111P} versus CMV-LacZ, $P < 0.05$). Also in mutant-transfected wounds, increased granulation tissue formation and re-epithelialization contributed to improved healing, and the extent of this response was comparable to that in wild-type-transfected wounds (Figure 5B; CMV-VEGF165-Wt versus CMV-LacZ, $P < 0.05$; CMV-VEGF165^{A111P} versus CMV-LacZ, $P < 0.05$) (Figure 5C; CMV-VEGF165-Wt versus CMV-LacZ, $P < 0.02$, CMV-VEGF165^{A111P} versus CMV-LacZ, $P < 0.05$). This data demonstrates the activity of the plasmin-resistant VEGF165 mutant *in vivo*. In our experimental model the VEGF165 mutant has a similar potency to the wild-type inducing early granulation tissue.

VEGF165^{A111P} Increases Vessel Size and the Stability of Vascular Structures during the Late Phase of Healing

To characterize the cellular composition within the granulation tissue formed, serial sections of wound tissues treated with VEGF165 were examined by immunohistochemistry. Morphometric quantification of the endothelial cell marker proteins CD31 and VEGFR-2 was used as read-out for neoangiogenic processes at the wound site (Figures 6 and 7); macrophages were identified by staining for the macrophage-specific antigen F4/80 (data not shown). Whereas CD31 is constitutively expressed in vascular endothelium, VEGFR-2 is highly expressed in vascular endothelial cells actively involved in capillary sprouting. Control methylcellulose-treated or CMV-LacZ-transfected wounds developed minimal cellular infiltrate and vascularized granulation tissue up to day 5 after wounding. Also epithelial wound edges showed no sign of hyperproliferation characteristic for wound edge-keratinocytes actively involved in re-epithelialization processes. After day 5, wounds started to be invaded by mononuclear inflammatory cells, spindle-shaped cells consistent with a fibroblast phenotype, and capillaries; epithelial wound edges thickened and fine epithelial tongues covered the newly formed granulation tissue (Figure 6, D and E). Granulation tissue formation eventually increased during the course of healing, reaching its maximum shortly before re-epithelialization was completed and was resolved thereafter. In contrast, experimental wounds treated topically with rhVEGF165 protein or transfected with either CMV-VEGF165-Wt or CMV-VEGF165^{A111P} constructs already showed an increased cellular infiltrate by day 5 after wounding. By day 8 a thick, highly cellular and vascularized granulation tissue had developed and capillary density was significantly increased in experimental wounds when compared to control wounds (Figure 6, A–C; rhVEGF165 versus control, $P < 0.05$; CMV-VEGF165-Wt versus CMV-LacZ, $P < 0.03$; CMV-VEGF165^{A111P} versus CMV-LacZ, $P < 0.003$). At this time point small VEGFR-2-positive capillaries were scattered throughout the granulation tissue area indicating neoangiogenesis (Figure 6G; rhVEGF165 versus control, $P < 0.03$; CMV-VEGF165-Wt versus CMV-LacZ, $P < 0.02$; CMV-VEGF165^{A111P} versus CMV-LacZ, $P < 0.02$). Epithelial wound edges were hyperproliferative at day 3 and the formation of epithelial tongues rapidly progressed over the freshly formed granulation tissue until wound closure was complete. The amount of granulation tissue and neovascularization was comparable in wounds treated topically with rhVEGF165 protein or transfected with CMV-VEGF165-Wt or CMV-VEGF165^{A111P} constructs, until the maximum was reached at day 8 after injury (Figure 5B and Figure 6, F and G). Although during the formation of granulation tissue the vessel density was comparable in wild-type- and mutant-treated wounds, the vessel size was significantly enlarged in mutant- versus wild-type-treated wounds 8 and 12 days after wounding (Figure 6H, $P < 0.03$). After day 8 density of CD31- and VEGFR-2-positive capillaries decreased in all experimental wounds, reflecting the transition between late granulation tissue and early scar formation (Figure 6F and Figure 7, G and H). Interestingly, during this late phase of healing, significant differences in capillary density became evident between wounds transfected with CMV-VEGF165-Wt or CMV-VEGF165^{A111P} expression constructs. When re-epithelialization was complete, at days 12 and 18 after wounding, capillary density was significantly increased in CMV-VEGF165^{A111P}- versus CMV-VEGF165-Wt-transfected wounds (Figure 7) ($P < 0.003$). At day 18 in CMV-VEGF165^{A111P}-transfected wounds CD31- and VEGFR-2-positive capillary structures were easily detectable in an early scar tissue. At this time point

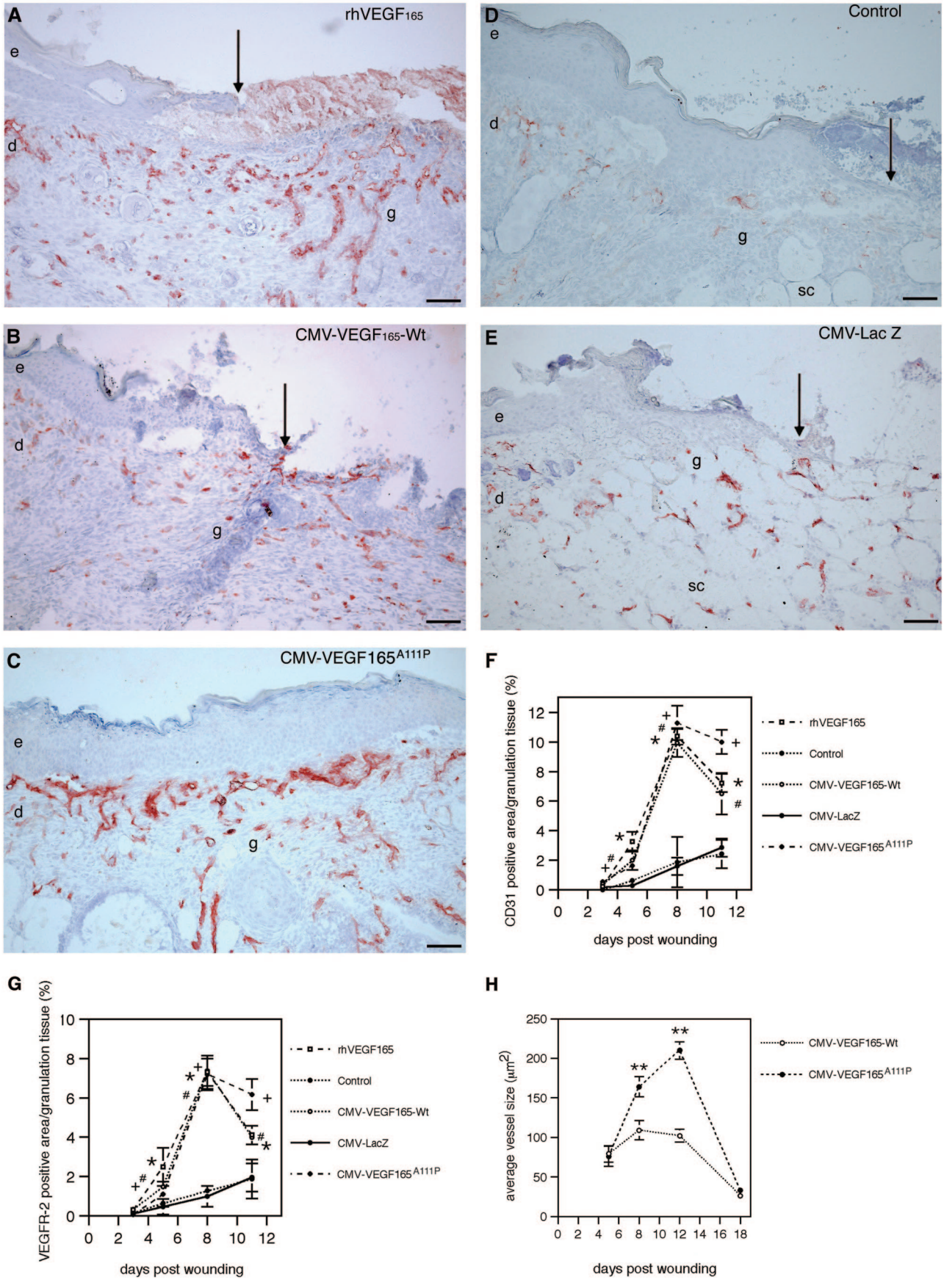
A
rhVEGF165
e
d
g
D
Control
e
d
g
sc
B
CMV-VEGF165-Wt
e
d
g
E
CMV-Lac Z
e
g
d
sc
C
CMV-VEGF165A111P
e
d
g
F
CD31 positive area/granulation tissue (%)
days post wounding
rhVEGF165
Control
CMV-VEGF165-Wt
CMV-LacZ
CMV-VEGF165A111P
G
VEGFR-2 positive area/granulation tissue (%)
days post wounding
rhVEGF165
Control
CMV-VEGF165-Wt
CMV-LacZ
CMV-VEGF165A111P
H
average vessel size (μm2)
days post wounding
CMV-VEGF165-Wt
CMV-VEGF165A111P

in CMV-VEGF165-Wt-transfected wounds, almost no capillaries were detectable (Figure 7D). This data demonstrates that vessel regression is delayed and reduced in VEGF165 mutant- versus wild-type-treated wounds and suggests an increased stability of vascular structures in mutant versus wild-type-treated wounds.

Pericyte Recruitment Is Increased and Capillary Endothelial Cell Apoptosis Is Delayed and Reduced in VEGF165^{A111P}-Transfected Wounds

To investigate whether reduced endothelial cell apoptosis contributes to the prolonged vessel persistence in CMV-VEGF165^{A111P}- versus CMV-VEGF165-Wt-transfected wounds we performed immunofluorescent double labeling of serial tissue sections where endothelial cells were identified by CD31 stain (red) and apoptotic cells by TdT mediate incorporation of dUTP into fragmented DNA (TUNEL) (green). In CMV-VEGF165-Wt- and CMV-VEGF165^{A111P}-transfected wounds at day 12, TUNEL staining alone revealed apoptotic cells scattered through the granulation tissue and the upper layer of the epidermis (Figure 8A). Double labeling of TUNEL with CD31 demonstrated that at day 12 the number of CD31-positive cells that were TUNEL-positive was significantly greater in CMV-VEGF165-Wt-transfected wounds than CMV-VEGF165^{A111P}-transfected wounds (Figure 8B) ($P < 0.01$). This data indicates that during granulation tissue resolution the number of apoptotic endothelial cells is decreased in CMV-VEGF165^{A111P}- versus CMV-VEGF165-Wt-transfected wounds, corroborating the increased stability of vascular structures in mutant- versus wild-type-treated wounds. At day 18 after transfection the number of apoptotic endothelial cells increased also in mutant-transfected wounds. Thus, VEGF165^{A111P} appeared to delay, but not prevent, normal regression of granulation tissue associated with granulation tissue maturation into scar.

To investigate the hypothesis that increased vessel stability in mutant-treated wounds was mediated by enhanced coating of vascular structures by perivascular cells, we performed a double-immunofluorescent labeling in which endothelial cells were identified by immunohistochemistry for CD31 (red) and perivascular cells by either desmin (green) or α-SMA (data not shown). In VEGF165 mutant-treated wounds, desmin-positive cells that associated or co-localized with vascular structures, could be easily identified at days 12 and 18 after wounding (Figure 9). In contrast, in VEGF165 wild-type-treated wounds, desmin expression was weak, and association of desmin-positive cells with vascular structures was rare 12 days after wounding. At day 18 the absolute number of vascular structures was dramatically reduced; however, remaining vessels were coated with desmin-positive perivascular cells. When analyzed by computer-assisted morphometric analysis, at day 12 both the absolute number of desmin-positive cells ($P < 0.001$) as well as the number of CD31-positive vessels associated with desmin-positive cells ($P < 0.001$) was significantly increased in mutant- versus wild-type-treated wounds (Figure 9, B and C). In addition, pericytes were identified by immunohistochemistry for α-SMA and the morphological and quantitative analysis of perivascular coating was confirmed. These results indicate that the plasmin-resistant VEGF165 mutant is more effective in recruiting perivascular cells, which ultimately mediate the increased vascular stability of newly formed blood vessels.

Discussion

Our results provide several lines of evidence to support the concept that the proteolytic microenvironment could function as a critical determinant controlling VEGF-A-mediated activities. Our study provides three new findings. First, in the db/db mouse the generation of plasmin activity is increased at the wound site during repair when compared with C57BL/6 mice. Second, in this model the stability of a mutant VEGF165 resistant to plasmin proteolysis is substantially increased in wound tissue lysates in comparison to VEGF165 wild type. Third, increased stability of VEGF165 had significant consequences to blood vessel persistence during the late phase of healing due to increased recruitment of perivascular cells and delayed and reduced endothelial cell apoptosis. To our knowledge this is the first report demonstrating in an *in vivo* model that VEGF165 proteolysis modulates VEGF-mediated angiogenesis.

The db/db mouse is characterized by a single autosomal recessive mutation in the leptin receptor gene (ObR), resulting into a phenotype similar to those of human adult-onset diabetes.[25] Cutaneous wound repair is severely impaired in db/db mice. Although, cellular and molecular mechanisms leading to the impaired healing response in this model are not clear, the sequelae of the loss of leptin receptor signaling including hyperglycemia, increased matrix metalloproteinase activity, and/or a prolonged inflammatory response at the wound site have been proposed as relevant pathomechanisms.[26–28] Recently, impaired healing in this model has been associ-

Figure 6. Vascular density is increased in VEGF165-treated wounds in db/db mice. Representative immunofluorescent staining demonstrates CD31-stained blood vessels (red) 8 days after wounding. Pronounced increase of microvascular density in granulation tissue of wounds treated topically with rhVEGF165 protein (**A**) or transfected with CMV-VEGF165-Wt (**B**) or CMV-VEGF165^{A111P} (**C**) expression constructs. Note that mutant-transfected wound shows a hyperproliferative epithelium, which just reached complete re-epithelialization. Significantly reduced granulation tissue and microvascular density in granulation tissue of methylcellulose-treated (control) (**D**) or CMV-LacZ-transfected (**E**) wounds. Note that due to the lack of granulation tissue in control and CMV-LacZ-treated wounds the subcutaneous fat tissue, which is abundant in db/db mice, is visible beneath the epithelial wound edges. Blood vessels stained in CMV-LacZ-treated wounds are localized in the subcutaneous fat tissue. Time course of computer-assisted morphometric analysis of CD31-positive cells (**F**) or VEGFR-2-positive cells (**G**) within the granulation tissue. **H:** Average vessel size is increased in CMV-VEGF165^{A111P}- versus CMV-VEGF165-Wt-transfected wounds. Wounds are $n = 8$/time point for each treatment modality; data are expressed as mean ± SD (rhVEGF165 versus control, $^{*}P < 0.05$; CMV-VEGF165-Wt versus CMV-LacZ, $^{\#}P < 0.03$; CMV-VEGF165^{A111P} versus CMV-LacZ, $^{+}P < 0.003$; CMV-VEGF165-Wt versus CMV-VEGF165^{A111P}, $^{**}P < 0.03$). e, epidermis; d, dermis; sc, subcutaneous tissue; g, granulation tissue. **Arrows** indicate epithelial wound edge. Scale bars, 100 μm.

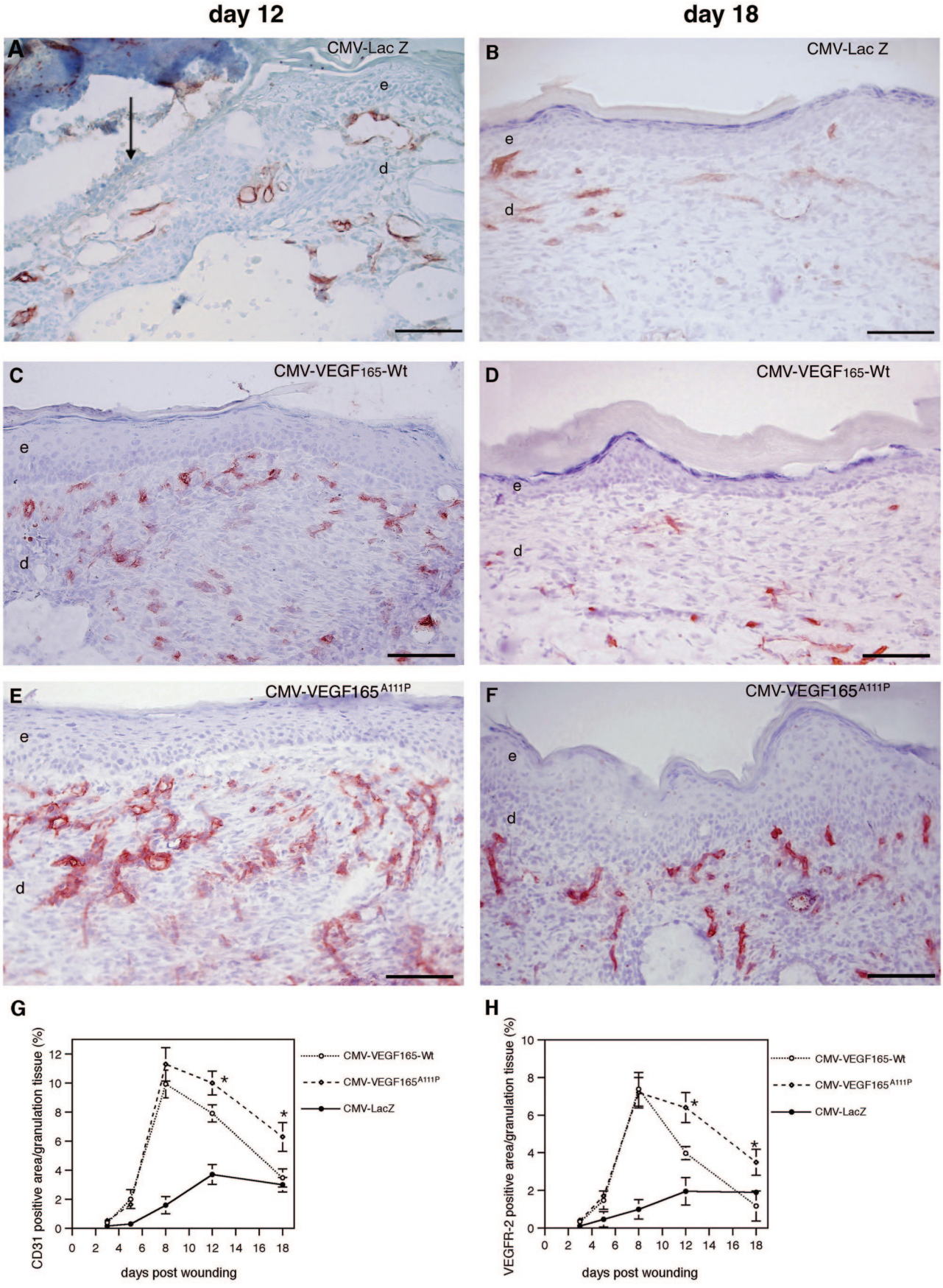
day 12
day 18
A
CMV-Lac Z
e
d
B
CMV-Lac Z
e
d
C
CMV-VEGF165-Wt
e
d
D
CMV-VEGF165-Wt
e
d
E
CMV-VEGF165A111P
e
d
F
CMV-VEGF165A111P
e
d
G
CD31 positive area/granulation tissue (%)
days post wounding
CMV-VEGF165-Wt
CMV-VEGF165A111P
CMV-LacZ
H
VEGFR-2 positive area/granulation tissue (%)
days post wounding
CMV-VEGF165-Wt
CMV-VEGF165A111P
CMV-LacZ

ated with a dramatically reduced angiogenic response. Lack of VEGF-A mRNA expression and disturbed intracellular VEGF-A protein processing indicate that VEGF-A protein deficiency is in part responsible for the regressive endothelial response observed in db/db mice.[28–30] Our data provide direct evidence that the delayed healing phenotype in db/db mice can be reversed by the local treatment of wounds with VEGF165-Wt protein or transfection using VEGF165-Wt plasmid cDNA. Interestingly, it has been reported recently that healthy transgenic mice overexpressing VEGF-A in the epidermis show no difference in wound closure rate when compared to their wild-type littermates.[31] Thus, our results illustrate the importance of using an impaired healing model for testing the effects of VEGF in tissue repair.

We chose the particle-mediated gene transfer technology, a physical means of gene delivery, to overexpress VEGF165 variants at the wound site. We and others have demonstrated that this technology provides an excellent experimental tool for the discovery and validation of novel gene products in skin.[21–23] In the present study wounds transfected with CMV-VEGF165-Wt cDNA showed an accelerated healing response comparable to wounds treated topically with recombinant hVEGF165 protein. These results confirm previous findings demonstrating that particle-mediated cutaneous *in vivo* transfection results in a biological response comparable with that obtained with the topical application of the corresponding recombinant growth factor.[21–23] The sustained expression of the transgene during the first week of healing and a more physiological delivery of the protein into the surrounding wound tissue are potential mechanisms resulting in the superior bioavailability of the transgene product.[23] Although we did not directly measure human VEGF165 in this study, previous estimates of luciferase expression with this technique estimated a steady-state of ~15 ng of gene product to be present in tissue homogenates.[21] Thus, our data indicates that small amounts of VEGF165 at the wound site are sufficient to provoke an angiogenic response and support recent findings indicating that even small variations in levels of VEGF expression have profound effects on vascularization.[32,33] Recently, Galiano and colleagues[19] demonstrated that topical rhVEGF165 can accelerate wound repair in the db/db mouse. However, in this model wounds were treated repetitively with high doses of rhVEGF165 protein (20 μg). These authors demonstrated that one effect of the peptide was the mobilization and recruitment of bone marrow-derived cells into the wound site, suggesting a systemic effect of the locally applied protein on wound repair. Although we did not analyze systemic effects, in our model, it is more likely that low VEGF165 doses expressed at the wound site act locally. Therefore, our data provide new information concerning the dosing of VEGF165-mediated angiogenesis in cutaneous wound repair.

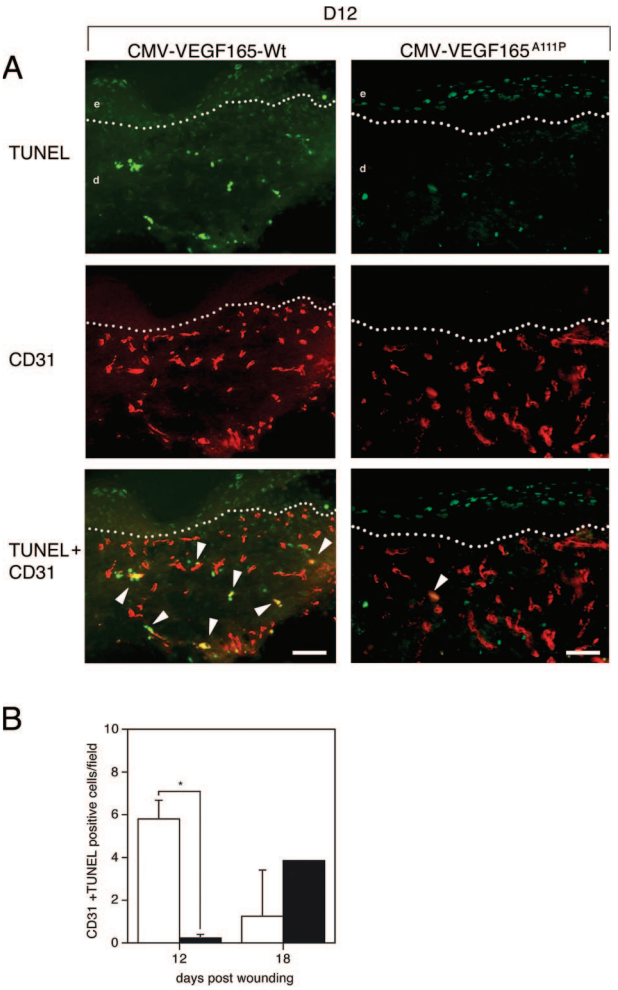

Figure 8. Reduced and delayed endothelial cell apoptosis in VEGF165^{A111P}-transfected wounds. **A:** Immunofluorescent staining of wounds 12 days after wounding. In CMV-VEGF165-Wt- or CMV-VEGF165^{A111P}-transfected wounds, TUNEL staining revealed apoptotic cells scattered through the granulation tissue and the upper layer of the epidermis. Double labeling of TUNEL with CD31 indicated that co-localization of both signals occurred at a significantly higher number in CMV-VEGF165-Wt- compared to CMV-VEGF165^{A111P}-transfected wounds (**white arrows** indicate CD31/TUNEL double-labeled cells). **B:** CD31- and TUNEL-positive cells were quantified in granulation tissue of CMV-VEGF165-Wt- (**white bars**) or CMV-VEGF165^{A111P}-transfected (**black bars**) wounds at indicated time points. Positive cells were analyzed in three individual fields per wound at ×600 magnification. Wounds are n = 4/time point for each treatment modality. Data are expressed as mean ± SD. **Dotted line** indicates the epidermal-dermal junction (CMV-VEGF165-Wt versus CMV-VEGF165^{A111P}, $^*P < 0.01$). e, epidermis; d, dermis. Scale bars, 100 μm.

Figure 7. Persistence of increased microvascular density in CMV-VEGF165^{A111P}-transfected wounds. Representative immunofluorescent staining demonstrates CD31-stained blood vessels (red) 12 and 18 days after wounding. **A** and **B:** Poorly vascularized granulation tissue in CMV-LacZ-transfected wounds. Note that blood vessels stained in CMV-LacZ-treated wounds are predominantly localized in the subcutaneous fat tissue. Pronounced induction of neovascularization in granulation tissue of wounds transfected with CMV-VEGF165-Wt (**C**) or CMV-VEGF165^{A111P} (**E**) expression constructs 12 days after wounding. **D:** Significantly reduced microvascular density in granulation tissue of CMV-VEGF165-Wt-transfected wounds at day 18 after wounding. **F:** Increased microvascular density in granulation tissue of CMV-VEGF165^{A111P}-transfected wounds persists until day 18 after wounding. **G:** Computer-assisted morphometric analysis of CD31-stained (**G**) or VEGFR-2-stained (**H**) wound sections revealed a significantly prolonged persistence of capillaries in granulation tissue of CMV-VEGF165^{A111P}-transfected wounds at days 12 and 18 after wounding when compared with CMV-VEGF165-Wt-transfected wounds. Wounds are n = 8/time point for each treatment modality; data are expressed as mean ± SD (CMV-VEGF165-Wt versus CMV-VEGF165^{A111P}, $^*P < 0.003$). e, epidermis; d, dermis. Scale bars, 100 μm.

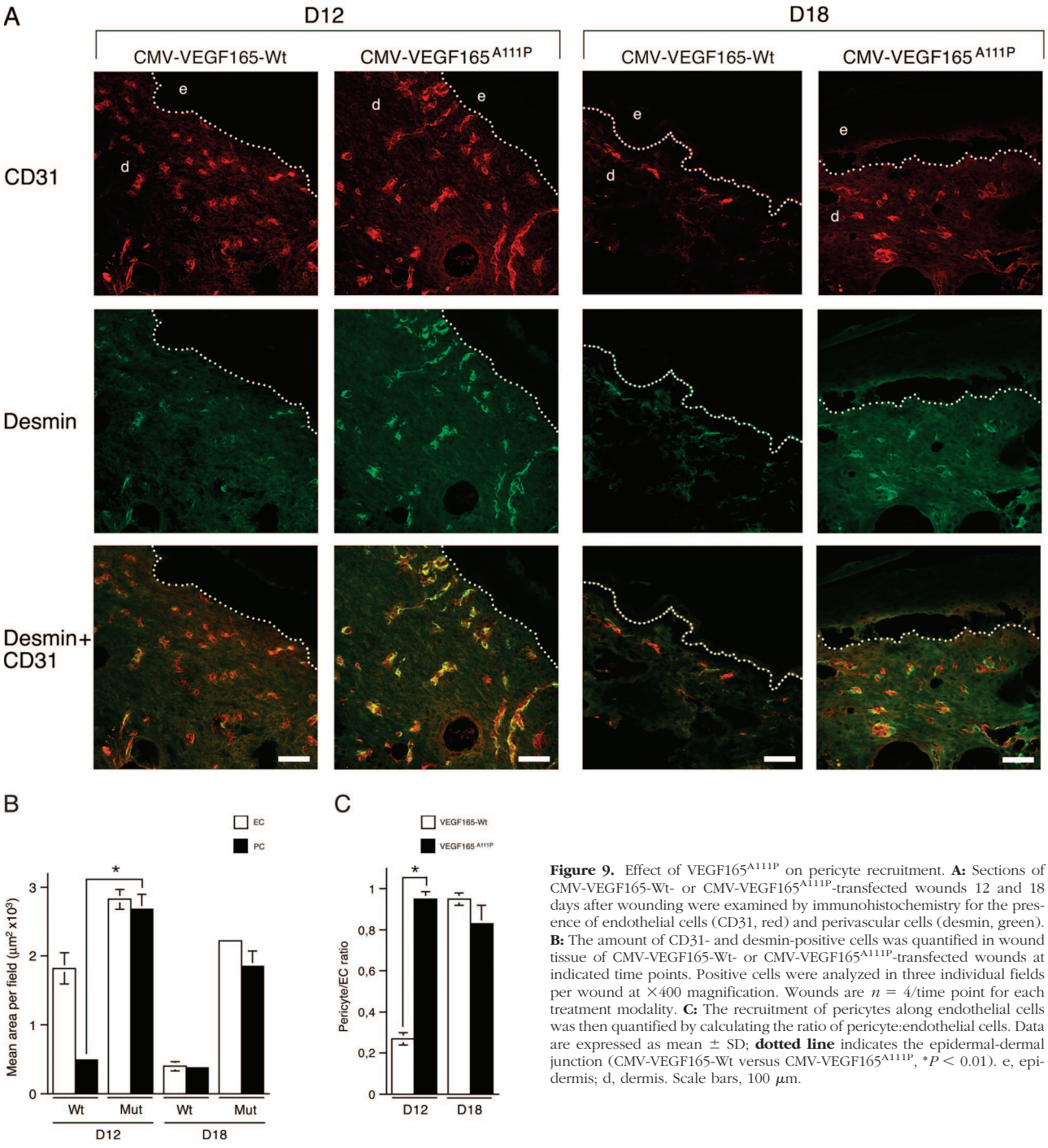

Figure 9. Effect of VEGF165^{A111P} on pericyte recruitment. **A:** Sections of CMV-VEGF165-Wt- or CMV-VEGF165^{A111P}-transfected wounds 12 and 18 days after wounding were examined by immunohistochemistry for the presence of endothelial cells (CD31, red) and perivascular cells (desmin, green). **B:** The amount of CD31- and desmin-positive cells was quantified in wound tissue of CMV-VEGF165-Wt- or CMV-VEGF165^{A111P}-transfected wounds at indicated time points. Positive cells were analyzed in three individual fields per wound at ×400 magnification. Wounds are $n = 4$/time point for each treatment modality. **C:** The recruitment of pericytes along endothelial cells was then quantified by calculating the ratio of pericyte:endothelial cells. Data are expressed as mean ± SD; **dotted line** indicates the epidermal-dermal junction (CMV-VEGF165-Wt versus CMV-VEGF165^{A111P}, $^*P < 0.01$). e, epidermis; d, dermis. Scale bars, 100 µm.

Histological and functional data indicate that the improved healing response after VEGF165 application is based on the induction of a highly vascularized granulation tissue as well as an accelerated re-epithelialization processes. The restricted distribution of VEGF receptors on endothelial cells and macrophages during cutaneous repair suggests that both direct VEGF receptor-mediated and indirect effects mediated by additional healing-related factors might be responsible for the improved healing response. The increased density of VEGFR-2-positive capillaries detected within the granulation tissue of VEGF165-Wt-treated wounds strongly supports a direct effect of the topically applied VEGF165-Wt on vascular endothelium. First, VEGF165 is one of the major inducers for endothelial VEGFR-2 expression.[34] Second, VEGFR-2 expression identifies endothelial cells actively involved in capillary sprouting.[35,36] Further, numerous macrophages could be identified within the granulation tissue of VEGF165-Wt-treated wounds, and VEGFR-1 signaling provides a strong chemotactic signal for macrophages.[37] VEGF receptors are absent on keratinocytes, and increased re-epithelialization of VEGF165-Wt-treated

wounds suggests that paracrine effects mediated by the underlying cellular and highly vascularized granulation tissue contribute to the augmented re-epithelialization response in VEGF165-Wt-treated wounds. Therefore, our data indicate that local VEGF165-Wt treatment can induce a highly vascularized, functionally active granulation tissue in db/db mice, supporting re-epithelialization processes.

Wounds transfected with VEGF165^{A111P} cDNA, coding for a plasmin-resistant VEGF165 variant, provoked an early granulation tissue formation, which in regard to the vessel density and cellular composition was similar to that induced by the wild-type molecule. However, vessel size was significantly increased in mutant- versus wild-type-treated wounds 8 and 12 days after wounding. Enlargement of vessel diameter is a typical feature for VEGF165-mediated angiogenesis and supports the hypothesis that in the protease-rich wound environment the angiogenic potency of the VEGF165 mutant is increased.[38] Nevertheless, differences in vessel size did not affect wound closure rate, which was similar in VEGF165-Wt- and VEGF165^{A111P}-transfected wounds. It is conceivable that during the initial phase after wound transfection, transgene expression is high, so that differences between the effects of VEGF165-Wt and mutant on vascular density were masked because of excess of VEGF165 molecules. However, we found significant differences regarding vessel regression in VEGF165-Wt- and mutant-transfected wounds during later stages in the repair process. In wild-type-transfected wounds capillary density resolved rapidly on completion of wound re-epithelialization, whereas VEGF165A^{111P}-transfected wounds were characterized by a significantly delayed involution of capillary density after wound closure. This finding was consistent with a delayed and decreased number of apoptotic endothelial cells in VEGF165^{A111P}-transfected wounds when compared to VEGF165-Wt-transfected wounds, and it suggests an increased stability of vascular structures in VEGF165-mutant- versus VEGF165-Wt-treated wounds.

VEGF-A is a critical survival factor for vascular endothelium, in particular for immature vessels.[9,39,40] The decreased endothelial cell apoptosis observed in mutant-treated wounds may therefore have resulted from an increased stability and prolonged local activity of the VEGF165 mutant. This assumption was supported by Western blot analysis and CD31/TUNEL analysis, which demonstrated increased stability and activity of the VEGF165 mutant within a highly proteolytic wound environment. In addition, our data indicate that capillaries induced by the VEGF mutant are characterized by an increased coating of perivascular cells. VEGF165 is chemotactic for pericytes, and in various models of angiogenic remodeling ectopic application of VEGF-A has been shown to accelerate pericyte coverage of newly formed blood vessels, which ultimately increased vessel maturation.[39,41,42] Therefore, the prolonged vessel persistence in VEGF165^{A111P}-transfected wounds might result from a combination of prolonged local VEGF165 mutant activity and increased pericyte coating.

Different structural-functional properties of the VEGF165 mutant and the wild-type protein could account for the prolonged and enhanced activity of the mutant. We and others have demonstrated that plasmin-catalyzed cleavage of VEGF165 results in loss of its heparin-binding domain.[12,14,15] The heparin-binding domain is crucially involved in diverse biochemical and functional properties of VEGF-A.[4–10] Inactivation of the plasmin cleavage site should lead to the preservation/integrity of the heparin-binding domain in the VEGF165 molecule, which enhances VEGF-receptor-affinity and/or extracellular matrix interactions. The VEGF-A heparin-binding domain has been identified as the epitope for neuropilin-1 (Nrp-1) binding.[8] Although endothelial VEGF-A signaling described to date is primarily mediated via VEGFR-1 and/or -2, its mitogenic, migratory, and survival signaling can be significantly facilitated by signaling through the membrane-bound co-receptor Nrp-1.[8,43] In addition, the heparin-binding domain of VEGF-A isoforms is crucial for determining its binding to extracellular matrix molecules.[4,5] Recent data have demonstrated that the angiogenic potential of matrix-associated isoforms is superior to soluble isoforms.[44] Overall, effects mediated by the heparin-binding domain may act separately and/or in concert to enhance and prolong the activity of the plasmin-resistant VEGF165 molecule in the db/db wound environment.

Our present data provide experimental evidence that a plasmin-resistant VEGF165 variant exerts increased stability in the highly proteolytic environment of an impaired healing wound with significant consequences to blood vessel persistence. Future studies will have to investigate whether VEGF165 proteolysis, in particular plasmin-mediated proteolysis, also regulates VEGF165 activity in other physiological or pathological situations of angiogenesis. Beside unraveling novel regulatory mechanisms in VEGF-A physiology, our results may have a clinical impact. In the highly proteolytic environment of the non-healing human wound, the plasmin-resistant VEGF165 mutant is more effective in protecting newly formed capillaries.

Acknowledgment

We thank Carien Niessen for critically reading the manuscript and an instructive discussion.

References

1. Ferrara N, Gerber HP, LeCouter J: The biology of VEGF and its receptors. Nat Med 2003, 9:669–676
2. Tischer E, Mitchell R, Hartmann T, Silvia M, Gospodarowicz D, Fiddes JC, Abraham JA: The human gene for VEGF. J Biol Chem 1991, 266:11947–11954
3. Keyt BA, Nguyen HV, Berleau LT, Duarte CM, Park J, Chen H, Ferrara N: Identification of vascular endothelial growth factor determinants for binding KDR and FLT-1 receptors. J Biol Chem 1996, 271:5638–5646
4. Park J, Keller GA, Ferrara N: The VEGF isoforms: differential deposition into the subepithelial extracellular matrix and bioactivity of extracellular matrix bound VEGF. Mol Biol Cell 1993, 4:1317–1326

5. Ortega N, L'Faqihi FE, Plouet J: Control of VEGF activity by the extracellular matrix. Biol Cell 1998, 90:381–390
6. Carmeliet P, Ng YS, Nuyens D, Theilmeier G, Brusselmans K, Cornelissen I, Ehler E, Kakkar VV, Stalmans I, Mattot V, Perriard JC, Dewerchin M, Flameng W, Nagy A, Lupu F, Moons L, Collen D, D'Amore PA, Shima DT: Impaired myocardial angiogenesis and ischemic cardiomyopathy in mice lacking the VEGF isoform VEGF164 and VEGF188. Nat Med 1999, 5:495–502
7. Hutchings H, Ortega N, Plouet J: Extracellular matrix-bound VEGF promotes endothelial cell adhesion, migration, and survival through integrin ligation. FASEB J 2003, 17:1520–1522
8. Soker S, Takashima S, Miao HQ, Neufeld G, Klagsbrun M: Neuropilin-1 is expressed by endothelial and tumor cells as isoform-specific receptor for VEGF. Cell 1998, 92:735–745
9. Dor Y, Djonov V, Abramovitch R, Itin A, Fishman GI, Carmeliet P, Goelman G, Keshet E: Conditional switching of VEGF provides new insights into adult neovascularization and pro-angiogenic therapy. EMBO J 2002, 21:1939–1947
10. Ruhrberg C, Gerhardt H, Golding M, Watson R, Ioannidou S, Fujisawa H, Betsholtz C, Shima DT: Spatially restricted patterning cues provided by heparin-binding VEGF-A morphogenesis. Gene Dev 2002, 16:2684–2698
11. Houck KA, Leung DW, Rowland AM, Winer J, Ferrara N: Dual regulation of VEGF bioavailability by genetic and proteolytic mechanisms. J Biol Chem 1992, 267:26031–26037
12. Keyt BA, Berleau LT, Nguyen HV, Chen H, Heinsoh H, Vandlen R, Ferrara N: The carboxyl-terminal domain (111-165) of VEGF is critical for its mitogenic potency. J Biol Chem 1996, 271:7788–7795
13. Plouet J, Moro F, Bertagnolli S, Coldeboeuf N, Mazarguil H, Clamens S, Bayard F: Extracellular cleavage of the VEGF189-amino acid form by urokinase is required for its mitogenic effect. J Biol Chem 1997, 272:13390–13396
14. Lauer G, Sollberg S, Cole M, Flamme I, Stürzebecher J, Mann K, Krieg T, Eming SA: Expression and proteolysis of VEGF is increased in chronic wounds. J Invest Dermatol 2000, 115:12–18
15. Lauer G, Sollberg S, Cole M, Krieg T, Eming SA: Generation of a novel proteolysis resistant VEGF 165 variant by a site-directed mutation at the plasmin sensitive cleavage site. FEBS Lett 2002, 531:309–313
16. Brown LF, Yeo KT, Berse B, Senger DR, Dvorak HF, Van De Water L: Expression of VEGF by epidermal keratinocytes during wound healing. J Exp Med 1992, 176:1375–1379
17. Nissen NN, Polverini PJ, Koch AE, Volin MV, Gamelli RL, DiPietro LA: VEGF mediates angiogenic activity during the proliferative phase of wound healing. Am J Pathol 1998, 152:1445–1452
18. Kishimoto J, Ehama R, Ge Y, Kobayashi T, Nishiyama T, Detmar M, Burgeson RE: In vivo detection of human VEGF promoter activity in transgenic mouse skin. Am J Pathol 2000, 157:103–110
19. Galiano RD, Tepper OM, Pelo CR, Bhatt KA, Calaghan M, Bastidas N, Bunting S, Steinmetz HG, Gurtner GC: Topical VEGF accelerates diabetic wound healing through increased angiogenesis and by mobilizing and recruiting bone marrow-derived cells. Am J Pathol 2004, 164:1935–1947
20. Rossiter H, Barresi C, Pammer J, Rendl M, Haigh J, Wagner EF, Tschachler E: Loss of VEGF A activity in murine epidermal keratinocytes delays wound healing and inhibits tumor formation. Cancer Res 2004, 64:3508–3516
21. Benn SI, Whitsitt JS, Broadly KN, Nanney LB, Perkins D, He L, Patel M, Morgan JR, Swain WF, Davidson JM: Enhancement of wound healing in rat skin following particle bombardment with cDNAs encoding TGF-b1. J Clin Invest 1996, 98:2894–2902
22. Eming SA, Whitsitt JS, He L, Krieg T, Morgan JR, Davidson JM: Particle-mediated gene transfer of PDGF isoforms promotes wound repair. J Invest Dermatol 1999, 112:297–302
23. Davidson JM, Krieg T, Eming SA: Particle-mediated gene therapy of wounds. Wound Rep Reg 2000, 8:452–459
24. Eming SA, Medalie DA, Tompkins RG, Yarmush ML, Morgan JR: Genetically modified human keratinocytes overexpressing PDGF-A enhance the performance of a composite skin graft. Hum Gene Ther 1998, 9:529–539
25. Lee GH, Proenca R, Montez JM, Carroll KM, Darvishzadeh JG, Lee JI, Friedman JM: Abnormal splicing of the leptin receptor in diabetic mice. Nature 1996, 379:632–635
26. Wetzler C, Kämpfer H, Stallmeyer B, Pfeilschifter J, Frank S: Large and sustained induction of chemokines during impaired wound healing in the genetically diabetic mouse: prolonged persistence of neutrophils and macrophages during the late phase of repair. J Invest Dermatol 2000, 115:245–253
27. Goova MT, Li J, Kislinger T, Qu W, Lu Y, Bucciarelli LG, Nowygrod S, Wolf BM, Caliste X, Yan SF, Stern DM, Schmidt AM: Blockade of receptor for advanced glycation end products restores effective wound healing in diabetic mice. Am J Pathol 2001, 159:513–525
28. Frank S, Hübner G, Breier G, Longaker MT, Greenhalgh DG, Werner S: Regulation of VEGF expression in cultured keratinocytes. J Biol Chem 1995, 270:12607–12613
29. Kämpfer H, Pfeilschifter J, Frank S: Expressional regulation of angiopoietin-1 and -2 and the Tie and -2 receptor tyrosine kinase during cutaneous wound healing: a comparative study of normal and impaired repair. Lab Invest 2001, 81:361–373
30. Ozawa K, Kondo T, Hori O, Kitao Y, Stern DM, Eisenmenger W, Ogawa S, Ohshima T: Expression of the oxygen-regulated protein ORP150 accelerates wound healing by modulating intracellular VEGF transport. J Clin Invest 2002, 108:41–50
31. Hong YK, Lange-Aschenfeld B, Velasco P, Hirakawa S, Kunstfeld R, Brown L, Bohlen P, Senger DR, Detmar M: VEGF-A tissue repair-associated lymphatic vessel formation via VEGFR-2 and the a1b1 and a2b1 integrins. FASEB J 18:1111–1113
32. Ozawa CR, Banfi A, Glazer NL, Thurston G, Springer ML, Kraft PE, McDonald DM, Blau HM: Microenvironmental VEGF concentration, not total dose, determines a threshold between normal and aberrant angiogenesis. J Clin Invest 2004, 113:516–527
33. Miquerol L, Langille BL, Nagy A: Embryonic development is disrupted by modest increases in VEGF gene expression. Development 2000, 127:3941–3946
34. Wang D, Donner DB, Warren RS: Homeostatic modulation of cell surface KDR and Flt1 expression and expression of the VEGF receptor mRNAs by VEGF. J Biol Chem 2000, 275:15905–15911
35. Millauer B, Wizigmann-Voos S, Schnürch H, Martinez R, Moller NP, Risau W, Ullrich A: High affinity VEGF binding and developmental expression suggest flk-1 as a major regulator of vasculogenesis and angiogenesis. Cell 1993, 72:835–846
36. Gerhardt H, Golding M, Fruttiger M, Ruhrberg C, Lundkvist A, Abramsson A, Jeltsch M, Mitchell C, Alitalo K, Shima D, Betsholtz C: VEGF guides angiogenic sprouting utilizing endothelial tip cell filopodia. J Cell Biol 2003, 161:1163–1177
37. Barleon B, Sozzani S, Zhou D, Weich HA, Mantovani A, Marme D: Migration of human monocytes in response to VEGF is mediated via the VEGF receptor flt-1. Blood 1996, 87:3336–3343
38. Sundberg C, Nagy JA, Brown LF, Feng D, Eckelhoefer I, Manseau EJ, Dvorak AM, Dvorak HF: Glomeruloid microvascular proliferation follows adenoviral VPF/VEGF-164 gene delivery. Am J Pathol 2001, 158:1145–1160
39. Alon T, Hemo I, Itin A, Peer J, Stone J, Keshet E: VEGF acts as a survival factor for newly formed retinal vessels and has implications for retinopathy of prematurity. Nat Med 1995, 10:1024–1028
40. Holash J, Maisonpierre PC, Compton C, Boland P, Alexander CR, Zagzag D, Yancopoulos GD, Wiegand SJ: Vessel cooption, regression, and growth in tumors mediated by angiopoietins and VEGF. Science 1999, 284:1994–1998
41. Grosskreutz CL, Anand-Apte B, Duplaa C, Quinn TP, Terman BI, Zetter B, D'Amore PA: VEGF-induced migration of vascular smooth muscle cells in vitro. Microvasc Res 1999, 58:128–136
42. Benjamin LE, Hemo I, Keshet E: A plasticity window for blood vessel remodeling is defined by pericyte coverage of the preformed endothelial network and is regulated by PDGF-B and VEGF. Development 1998, 125:1591–1598
43. Whitaker GB, Limberg BJ, Rosenbaum JS: VEGF receptor-2 and neuropilin-1 form a receptor complex that is responsible for the differential signaling potency of VEGF165 and VEGF121. J Biol Chem 2001, 276:25520–25531
44. Zisch AH, Lutolf MP, Ehrbar M, Raeber GP, Rizzi SC, Davies N, Schmokel H, Bezuidenhout D, Djonov V, Zilla P, Hubbell JA: Cell-demanded release of VEGF from synthetic, biointeractive cell ingrowth matrices for vascularized tissue growth. FASEB J 2003, 17:2260–2262